A portable dual-wavelength multichannel oximeter based on time-resolved reflectance spectroscopy

Rinaldo Cubeddu,[*] **Antonio Pifferi, Paola Taroni, Alessandro Torricelli and Gianluca Valentini**

INFM-Dipartimento di Fisica and Centro di Elettronica Quantistica e Strumentazione Elettronica (CEQSE)-CNR, Politecnico di Milano, Piazza Leonardo da Vinci 32, I-20133 Milan, Italy.
e-mail: rinaldo.cubeddu@fisi.polimi.it.

Introduction

In the wavelength range between 600 nm and 1200 nm (the so-called therapeuthic window) biological tissues are highly diffusive media.[1] This spectral region is, in fact, far enough from the dominant absorption peak of water at longer wavelengths and from the huge absorption peaks of hemoglobin and nucleic acids at the shorter wavelengths. Therefore, the scattering of light, caused by the microscopic discontinuities of the refractive index within tissue, is the main phenomenon which photons undergo when injected into tissue. Red and near infrared light can thus penetrate deeply into biological tissue, interact with its constituents and subsequently be remitted. Useful information on tissue functional state can thus be obtained. For example, the absorption of light by hemoglobin has been used since 1940 to monitor tissue oxygen consumption, on the basis of the different spectral features of oxygenated hemoglobin (HbO_2) and deoxygenated hemoglobin (Hb).[2] More recently, the tracking of light scattering changes with time has been proposed for non-invasively monitoring blood glucose levels[3,4] and fast signals in the brain cortex.[5–7]

However, quantitative monitoring of physiological functions requires the discrimination between absorption and scattering events of light in tissues. This can not be achieved by standard CW techniques, which are based on the measure of total attenuation and which, therefore, unavoidably mix absorption and scattering contributions. In recent years, space-, frequency- and time-resolved reflectance spectroscopy proved to be a valuable tool to non-invasively characterize tissue optical properties and to separate the effect of absorption and scattering.[8–10] Several prototypes and instruments based on space- and frequency-resolved reflectance spectroscopy have been developed and effectively used in basic laboratory demonstrations and in clinical practice. However, due to technological constraints, only a few time-resolved systems have been devised.[11]

In this paper we present the development of a dual-wavelength, multichannel, time-correlated single photon counting system for the non-invasive assessment of tissue absorption and reduced scattering. Preliminary results on volunteers demonstrate the possibility of non-invasively tracking tissue oxygenation in real time.

System set-up

Figure 1 shows the scheme of our system set-up. The light sources are two pulsed laser diodes (Model PDL800, PicoQuant GmbH, Germany) operating at 672 nm and 818 nm respectively, with a pulse repetition rate up to 80 MHz, an average power of 1 mW and a duration of about 100 ps. The rel-
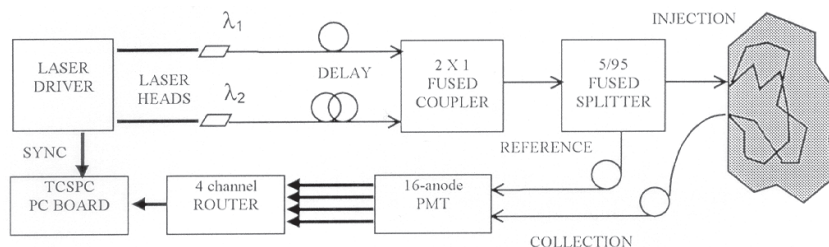
Figure 1. Scheme of the system set-up.

ative delay between the 818 nm and the 672 nm laser pulses is adjusted by means of a couple of optical fibres (Model MMF-IRVIS-50/125, OZ Optics, Canada), so that laser pulses are coupled together with no need for time-sharing. A small fraction (5%) of the laser beam is split off (Model FUSED IRVIS, OZ Optics, Canada) and fed directly into a multi-anode photomultiplier (Model R5600U-L16, Hamamatsu, Japan) to account for eventual time-drifts of the instrumentation and to provide a time-reference. A couple of 1 mm fibres (PCS1000W, Quartz et Silice, France) delivers and collects light from the sample. The reflectance photons are detected by the photomultiplier and the output signals are redirected by a router (Model HRT-41, Becker&Hickl GmbH, Germany) to different memory blocks of the TCSPC PC board (Model SPC-300, Becker&Hickl GmbH, Germany). A PC controls both data acquisition and data analysis. The typical instrument response function, obtained facing the injection and the collection fibres, has a FWHM of about 200 ps.

The solution of the time-dependent diffusion equation for the reflectance through a semi-infinite homogeneous medium[12] is first convoluted with the instrument response function and then best-fitted to the experimental curves, leading to the estimate of the reduced scattering and absorption coefficients (μ_s' and μ_a). Since both wavelengths are simultaneously injected into the sample and the corresponding time-resolved reflectance curves are simultaneously acquired, at each acquisition we get the estimates of μ_a and μ_s' at both wavelengths. The overall time for data analysis is 100 ms on a standard PC (Model Pentium 166 MHz, Intel).

Assuming oxyhaemoglobin (HbO$_2$) and deoxyhaemoglobin (Hb) as the only constituents contributing to the absorption and taking the extinction coefficient of Hb and HbO$_2$ from the literature,[13] we are able to obtain estimates of the oxygenated haemoglobin content [HbO$_2$] and of the deoxygenated haemoglobin content [Hb] so as to deduce the oxygen saturation fraction Y = [HbO$_2$] /([HbO$_2$] + [Hb]) and the total haemoglobin concentration THC = [HbO$_2$] + [Hb] .

Figure 2 shows a typical instrument response function (IRF, FWHM = 200 ps), a time-resolved reflectance curve (μ_a = 0.45 cm^{-1}, μ_s' = 16 cm^{-1}) and the theoretical curve provided by the diffusion theory.
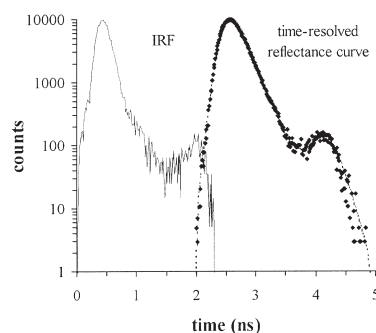

Figure 2. Instrument transfer function (IRF, FWHM = 200ps, continuous line) and time resolved reflectance curve (filled diamond: experimental data; dashed line: fit to solution provided by the diffusion theory). The optical parameters are μ_a = 0.45 cm^{-1}, μ_s' = 14.2 cm^{-1}, at 818 nm.

A more detailed description of the system set-up, together with system characterisation on realistic tissue phantoms made of Intralipid and ink and with a discussion on the fitting procedures can be found in Reference 14.

Experiments and results

Preliminary *in vivo* measurements of tissue oxygenation were performed on the medial aspect of the right arm, away from any palpable bone, on healthy volunteers, recruited from the laboratory. For time-resolved reflectance measurements, the injection and collection fibres were held naturally to the skin at a relative distance, $\rho = 2.0$ cm by a plastic black strip fastened with an elastic strap, so that they provided no pressure to the skin and no movement was allowed. The arm was wrapped in black cloth and measurements were performed in a dimmed room to decrease the amount of background light. The arm was placed in a comfortable resting position on a flat surface. A pneumatic cuff was placed loosely around the arm.

A standard protocol was followed. After an initial period (three minutes) in a resting position, the cuff was manually inflated to a pressure of 100 mm Hg to provide an abrupt venous occlusion, but no arterial occlusion. The cuff occlusion was maintained for five minutes with the muscle resting. The cuff was then released and the recovery phase followed for seven minutes. A second experiment was performed following the same protocol and with a cuff pressure of 250 mm Hg to provide both venous and arterial occlusion.

Figure 3 (top row) shows Y and THC as a function of time for the venous occlusion protocol. During venous occlusion, oxygenated blood is supplied to the muscle via the artery system, while
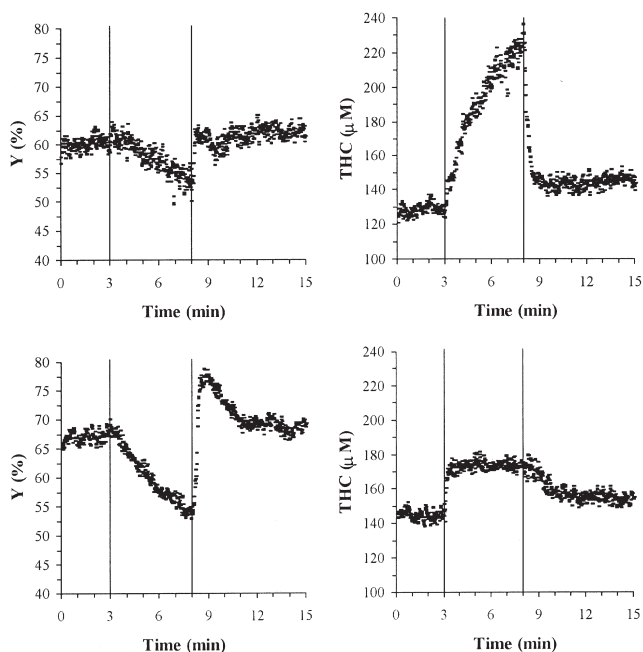

Figure 3. Tissue oxygen saturation fraction Y (left column) and total hemoglobin concentration THC (right column) as a function of time in the venous occlusion protocol (cuff pressure 100 mmHg, top row) and in the arterial occlusion protocol (cuff pressure 250 mm Hg, bottom row), respectively.

deoxygenated blood can not flow away via the venous system. At the same time, the muscle keeps burning oxygen. As a consequence, in the measured region, a large increase in THC (about 100 μM) and a minor decrease in Y (less than 10%) can be detected. Then, when cuff is released Y increases due to the flow of new oxygenated blood and THC presents a very steep decrease. Finally, both parameters return to values closer to the initial ones.

Figure 3 (bottom row) shows Y and THC as a function of time for the arterial occlusion protocol. During venous and arterial occlusion, no oxygenated blood is supplied to the muscle via the artery system and no deoxygenated blood flows away via the venous system but, at the same time, the muscle keeps burning oxygen. Thus, we observe, as expected, a decrease in Y (about 15%) followed by a huge increase (+ 30%) when cuff is released. Minor changes are reported in THC: a 30 μM increase when the cuff is inflated and a slow recovery to the initial value when the cuff is released.

Conclusion

We demonstrated the feasibility of tissue oxygenation measurements by using a compact time-resolved instrumentation based on the time-correlated, single-photon counting technique. Preliminary *in vivo* measurements of tissue oxygenation under different physiological conditions were performed on healthy volunteers.

Time-resolved reflectance curves were acquired every 100 ms. During the fitting procedures, data were obtained by averaging the results of 10 curves, resulting in an integration time of 1 s. Nonetheless, the possibility of acquiring data at such a fast sampling rate permits not only to be sensitive to fast physiological signals, but also to get rid of artifacts due to rapid sources of noise (for example, pulsation, respiration, or muscle contraction), thus further extending the potential applications of the system, as described in Reference 14.

The system can be modified easily to increase the number of illumination wavelengths, so that other chromophores, besides hemoglobin can be taken into account in the estimation of tissue oxygenation. Moreover, the use of multiple injection points will provide the spatial mapping of tissue oxygenation, thus, overcoming the heterogeneity of the sample and testing different regions simultaneously.

References

1. B. Chance and A. Yodh, *Phys. Today* **48,** 34 (1995) and references therein.
2. G.A. Millikan, *Rev. Sci. Instrum.* **13,** 434 (1942).
3. J.S. Maier, S.A. Walker, S. Fantini, M.A. Franceschini and E. Gratton, *Opt. Lett.* **19,** 2062 (1994).
4. M. Kohl, M. Cope, M. Essenpreis and D. Böckner, *Opt. Lett.* **19,** 2170 (1994).
5. G. Gratton, M. Fabiani, D. Friedman, M.A. Franceschini, S. Fantini, P.M. Corbellis and E. Gratton, *J. Cogn. Neurosc.* **7,** 446 (1995).
6. E. Gratton, S. Fantini, M.A. Franceschini, G. Gratton and M. Fabiani, *Phil. Trans. R. Soc. of London B* **352,** 727 (1997).
7. M. Kohl, U. Lindauer, U. Dirnagl and A. Villringer, "Investigation of cortical spreading depression in rats by near infrared spectroscopy", in *Advances in Optical Imaging and Photon Migration*, Technical Digest. Optical Society of America, Washington DC, USA, pp. 21–22 (1988).
8. T.J. Farrell, M.S. Patterson and B.C. Wilson, *Med. Phys.* **19,** 879 (1992).
9. M.S. Patterson, J.D. Moulton, B.C. Wilson, K.W. Berndt and J.R. Lakowitz, *Appl. Opt.* **30,** 4474 (1991).
10. M.S. Patterson, B. Chance and B.C. Wilson, *Appl. Opt.* **28,** 2331 (1989).
11. See for example: *Photon propagation in tissue III*, D.A. Benaron, B. Chance and M. Ferrari (Eds). SPIE Proc. Pp. 3194 (1998) and J.G. Fujimoto and M.S. Patterson, (Eds) *Advances in Optical Im-*

aging and Photon Migration, Vol. 21 of OSA Trends in Optics and Photonics Series. Optical So-
ciety of America, Washington, DC, USA (1998).

12. R.C. Haskell, L.O. Svaasand, T.T. Tsay, T.C. Feng, M.S. McAdams and B.J. Tromberg, *J. Opt. Soc. Am. A* **11,** 2727 (1994).
13. S.A. Prahl, *Biomedical Optics News* Etc, http://ece.ogi.edu/omlc/news, **June,** (1998).
14. R. Cubeddu, A. Pifferi, P. Taroni, A. Torricelli and G. Valentini, *Appl.Opt.* **38,** in press.